Proceedings of the 2012 IFAC Workshop on Automatic Control in Offshore Oil and Gas Production, Norwegian University of Science and Technology, Trondheim, Norway, May 31 - June 1, 2012



# Cascade Controller Including Backstepping for Hydraulic-Mechanical Systems

**Martin Choux** * **Geir Hovland** * **Mogens Blanke** **

* *Mechatronics Group, Department of Engineering, University of Agder, N-4892 Grimstad, Norway (e-mail: martin.choux@uia.no).*
** *Automation and Control Group, Department of Electrical Engineering, Technical University of Denmark, DK-2800 Kgs. Lyngby, Denmark (e-mail: mb@elektro.dtu.dk)*

**Abstract:**
Development of a cascade controller structure including adaptive backstepping for a nonlinear hydraulic-mechanical system is considered in this paper where a dynamic friction (LuGre) model is included to obtain the necessary accuracy. The paper compares the performance of two variants of an adaptive backstepping tracking controller with earlier results. The new control architecture is analysed and enhanced tracking performance is demonstrated when including the extended friction model. The complexity of the backstepping procedure is significantly reduced due to the cascade structure. Hence, the proposed control structure is better suited to real-time implementation.

*Keywords:* Hydraulic actuator, Lyapunov methods, Adaptive control

## 1. INTRODUCTION

Offshore oil and gas production relies in a large extend, today, on motion and force controlled hydraulic equipment. These nonlinear hydraulic-mechanical systems (NHMS) pose a significant challenge for model-based real-time control. Characteristics of typical models are: a) stiff with fast dynamics for the hydraulics and relatively slow dynamics for the mechanical parts, b) strong nonlinearities, for example valve overlap and input saturation, combined with dynamic elements occurring in orifice flow and in friction, c) non-measurable states (position and velocity of valves) and d)sensitivity to temperature and air content of oil characteristic parameters.

An experimental evaluation of ten different controller algorithms for an NHMS was presented in Bonchis et al. (2002). The results in the paper show that simple PI controller performed reasonably well, and only a few of the model-based controllers were able to improve performance.

Adaptive backstepping is a model-based nonlinear control technique that can be used for a class of systems with triangular structure in order to insure global asymptotical stability or tracking. A constructive design is presented by Kanellakopoulos et al. (1991) for feedback linearizable systems, later by Seto et al. (1994) and recent extensions for a larger class of systems by Pavlichkov and Ge (2009). It was recently applied to NHMS by Zeng and Sepehri (2006, 2008). The backstepping controller was not included in the survey of Bonchis et al. (2002). Hence, it is of interest to compare the backstepping and the PI controller for an NHMS. In Zeng and Sepehri (2006, 2008) the authors presented an adaptive controller to handle internal leakage and unknown friction in a cylinder, unknown volumes in the orifice equation and temperature dependent oil characteristics. However, a linearised valve model was used and no valve dynamics was considered.

The paper Choux and Hovland (2010) showed that valve dynamics can be significant and should be included in the model-based controller. In addition to the valve dynamics, the adaptive controller developed in Choux and Hovland (2010) also handled internal leakage and unknown friction in the cylinder, unknown volumes in the orifice equation and temperature dependent oil characteristics.

Another related work is the paper by Schindele and Aschemann (2009) where the authors consider backstepping control for a pneumatic system using a cascade control structure with feedforward friction compensation. The main differences between Schindele and Aschemann (2009) and the work presented here is the inner loop controller as well as the type of system (pneumatic vs. hydraulic-mechanical). Instead of using an inner loop containing valve characteristics and approximated inverse valve characteristics as in Schindele and Aschemann (2009), a PID controller is used in the inner loop together with a backstepping procedure in the outer loop.

One drawback of the paper Choux and Hovland (2010) was the relatively high complexity of the model-based backstepping controller and the difficulty in getting this controller to run fast enough on a real-time system. Hence, in this paper, the control structure is re-considered by introducing an internal PID control loop for the pressure in the cylinder. This change reduces the backstepping with three steps compared to the paper Choux and Hovland (2010). These are shown to be related to: pressure, valve position and velocity, and input voltage. Moreover, it is analysed how the friction model could be extended by including Stribeck effects, Coulomb friction and dynamic

phenomena (LuGre model, Canudas de Wit et al. (1995)) and better performance obtained as compared to linear viscous friction models.

## 2. MODEL DESCRIPTION

The same NHMS considered by Choux and Hovland (2010) and shown in Fig. 1 is used with similar values. Only the friction occuring in the cylinder is modelled using a more realistic approach when the dynamics effects of friction are considered. The tracking of the mass position $y$ in the NHMS shown in Fig. 1 is considered. Pressure sensors provide measurement of pressure difference between the two cylinder chambers $p_L$, also referred to as the load pressure, linear displacement sensor and velocity transducer (tachometer attached to a translation-rotation converting mechanism) measure the position $y$ and the velocity $\dot{y}$ of the mass element.

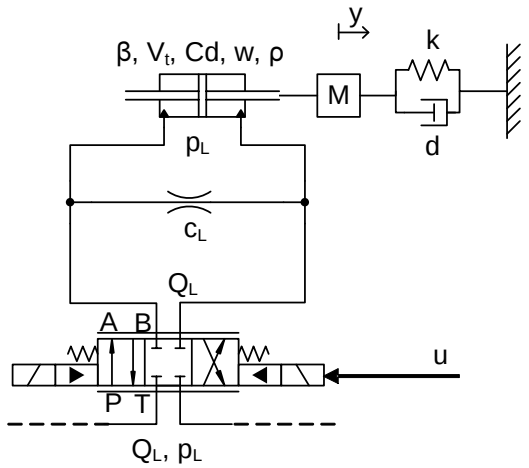


Fig. 1. Nonlinear hydraulic-mechanical system with control valve and hydraulic cylinder exerting forces on the object to be handled. Total load mass $M$, equivalent spring coefficient $k$ and damping $d$ are very uncertain.

New parameters for the dynamic friction model are given in Table 1.

### *2.1 LuGre Friction Model*

High friction inside the cylinder has significant effects in the performances of positon tracking. In order to compensate for Coulomb friction, Stribeck effect but also dynamic friction phenomena such as pre-sliding displacement and hysteresis, the LuGre model, described by the following equations is chosen:

$$F_{fric} = \sigma_0 z + \sigma_1 \dot{z} + \sigma_2 \dot{y} \tag{1}$$

$$\dot{z} = \dot{y} - \frac{|v|}{g(\dot{y})} z \tag{2}$$

$$g(\dot{y}) = \frac{F_c}{\sigma_0} + \frac{F_s - F_c}{\sigma_0} e^{-|\dot{y}|/v_s} \tag{3}$$

where $z$ is an internal state variable, $F_c$ is the Coulomb friction, $F_s$ the stiction force, $v_s$ the Stribeck velocity, $\sigma_0$ and $\sigma_1$ are the stiffness and damping coefficients and $\sigma_2$ is the viscous friction coefficient. Estimated values of these parameters, are given in Table 1.

Table 1. Values of the system parameters.

| Par. | Value | Par. | Value |
|---|---|---|---|
| $M$ | = 41 kg | $A$ | = 946 $mm^2$ |
| $k$ | = 65000 N/m | $d$ | = 500 Ns/m |
| $\sigma_0$ | = 5880 [N/m] | $\sigma_1$ | = 108 [Ns/m] |
| $\sigma_2$ | = 500 [Ns/m] | $F_c$ | = 100 [N] |
| $F_s$ | = 200 [N] | $v_s$ | = 0.001 [m/s] |

### *2.2 Uncertain parameters*

The moving mass $M$ which can be measured in an experimental test rig is nonetheless considered as uncertain in order to allow for a large range of applications as for example pick and place manipulation. Friction parameters, which can be identified with experiment contain also uncertainties due to different oil characteristics and wear inside the cylinder. Finally, the mechanical system contains uncertainties in the spring coefficient and damping coefficient. The adaptive controller presented in this paper handles all the uncertainties described above.

### *2.3 Assumptions*

Besides the assumption that friction can be modeled by a dynamical friction model (LuGre), the three following are also considered: The flow through the leakage between the two cylinder chambers is proportional to the load pressure (pressure difference between the two cylinder chambers). The spring and damper in the mechanical part are linear. Other assumptions concerning the valve nonlinearities and valve dynamics are not neccessary in the design of the controller thanks to the inner control structure developed in the next section.

## 3. CONTROLLER DESIGN

### *3.1 Trajectory initialization*

In order to improve the adaptation by making the uncertainty errors smaller and to improve the adaptive system's transient performance, the reference trajectory is initialized, see Krstić et al. (1995), such that the state variables are zero at time zero and the reference and its derivatives are continuous up to a certain order. In the simulation, the trajectory initialization is done using a Bessel low-pass filter of order 12 with a passband edge frequency of 150 rad/s.

### *3.2 Cascade controller with LuGre friction model compensation*

The position $y$ and velocity $\dot{y}$ of the mass and the load pressure $P_l$ are measured while the internal state $z_f$ of the friction model, not accessible by measurement, is estimated by a dual observer. One drawback of the controller in Choux and Hovland (2010) is the "explosion of terms" (see Alleyne and Liu (2000)), caused by the analytical differentiation of the stabilizing functions from one step to the next. If numerical differentiation is chosen instead, it can produce phase lag between synthetic inputs, requiring higher sampling rate and increases the number of algebraic loops in the simulation. In order to reduce the complexity of the controller and make it suitable for

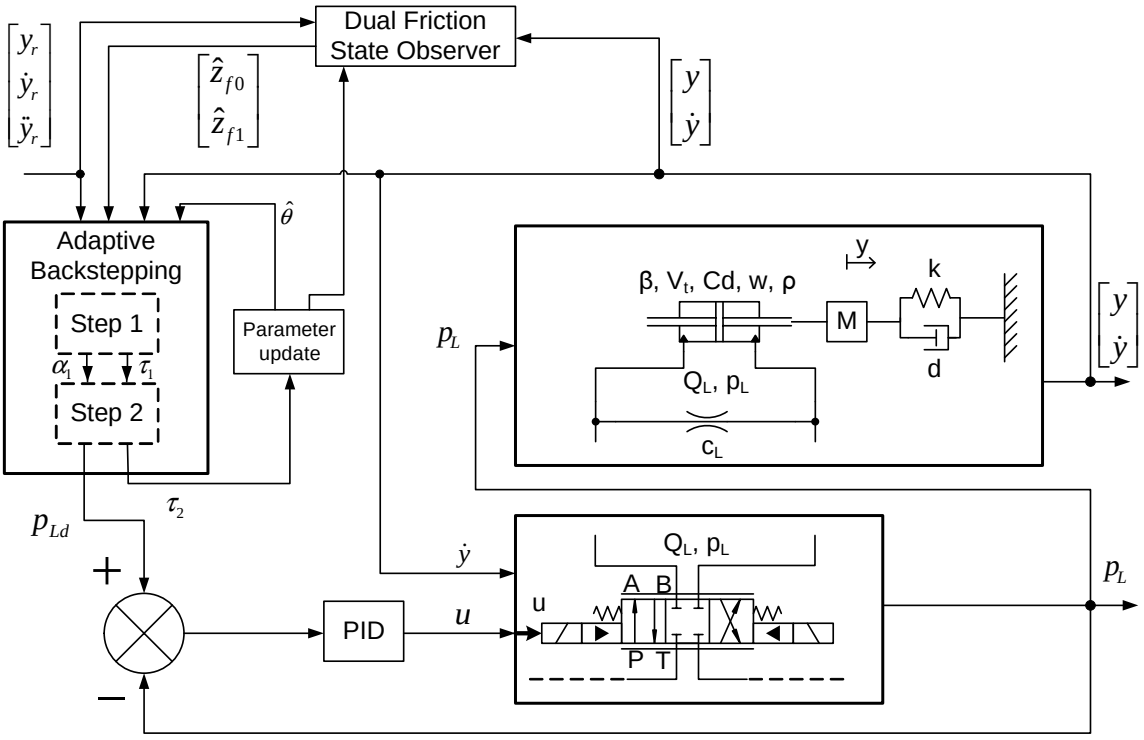


Fig. 2. Nonlinear controller.

real-time applications the backstepping design is stopped after two steps by considering the load pressure as the input. Using a cascade structure, as shown in Fig.2, the load pressure is controlled inside the inner loop by using a PID controller. The external loop ensures a perfect output reference tracking provided the internal loop works perfectly. Analysis of the inner pressure loop stability and performance is a topic for future research.

The following equations (in hydraulic units, for example $p_L$ in bar instead of Pa) describe the NHMS when $p_L$ is considered as the input:

$$\ddot{y} = -\frac{k}{M}y - \frac{d+\sigma_2+\sigma_1}{M}\dot{y} + \frac{A}{10M}p_L + \left(\frac{1}{M}\frac{\sigma_1\sigma_0\,|\dot{y}|}{F_c + (F_s - F_c)\exp\left(\frac{-|\dot{y}|}{v_s}\right)} - \frac{\sigma_0}{M}\right) z_f \quad (4)$$

$$\dot{z}_f = \dot{y} - \frac{\sigma_0|\dot{y}|}{F_c + (F_s - F_c)\exp\left(\frac{-|\dot{y}|}{v_s}\right)} z_f \quad (5)$$

Eq.(4) is acceleration of the actuator tool and the load mass, where $A$ is the cylinder effective area. If the state variables $[y, \dot{y}]$ are equal to $[x_1, x_2]$ and $p_{Ld} = p_L$, Eq.(4) can be rewritten as:

$$\dot{x}_1 = x_2 \quad (6)$$

$$\dot{x}_2 = \varphi(x_1, x_2)^T\theta + b\,p_{Ld} + \left(\beta_1\frac{|x_2|}{g(x_2)} - \beta_0\right) z_f \quad (7)$$

where the control coefficient $b = \frac{A}{10M}$ is unknown, $\theta$ is a vector of uncertain parameters:

$$\theta = [\theta_1, \theta_2]^T = \left[-\frac{k}{M}, -\frac{d+\sigma_1+\sigma_2}{M}\right]^T \quad (8)$$

and $\varphi(x_1, x_2)^T = [x_1 \;\; x_2]$, $g(x_2) = \frac{F_c}{\sigma_0} + \frac{F_s - F_c}{\sigma_0}\exp\left(\frac{-|x_2|}{v_s}\right)$, $\beta_1 = \frac{\sigma_1}{M}$, and $\beta_0 = \frac{\sigma_0}{M}$. Two observers are used to estimate the internal friction state $z_f$:

$$\left(\beta_1\frac{|x_2|}{g(x_2)} - \beta_0\right) z_f = \frac{|x_2|}{g(x_2)}\left(\beta_1\tilde{z}_{f1} + \tilde{\beta}_1\hat{z}_{f1} + \hat{\beta}_1\hat{z}_{f1}\right) - \beta_0\tilde{z}_{f0} - \hat{\beta}_0\hat{z}_{f0} - \tilde{\beta}_0\hat{z}_{f0} \quad (9)$$

and

$$\dot{\hat{z}}_{f0} = x_2 - \frac{|x_2|}{g(x_2)}\hat{z}_{f0} + \iota_0$$

$$\dot{\hat{z}}_{f1} = x_2 - \frac{|x_2|}{g(x_2)}\hat{z}_{f1} + \iota_1$$

where $\hat{z}$, $\tilde{z}$ represent the estimate of $z$ and $z - \hat{z}$, respectively. $\iota_{0,1}$ are correction terms that will be found in the next step.

Using the coordinate transformation:

$$z_1 = x_1 - y_r \quad (10)$$

$$z_2 = x_2 - \dot{y}_r - \alpha_1 \quad (11)$$

and the stabilizing functions:

$$\alpha_1 = -L_1 z_1 \quad (12)$$

$$\alpha_2 = -z_1 - L_2 z_2 - \varphi^T\hat{\theta} + \frac{\partial\alpha_1}{\partial x_1}x_2 + \frac{\partial\alpha_1}{\partial y_r}\dot{y}_r + \hat{\beta}_0\hat{z}_{f0} - \frac{|x_2|}{g(x_2)}\hat{\beta}_1\hat{z}_{f1} \quad (13)$$

the adaptive control law is given by:

$$p_{Ld} = \hat{\varrho}\,(\alpha_2 + \ddot{y}_r) \quad (14)$$

where $\hat{\varrho}$ is the estimate of $\varrho = \frac{1}{b}$ computed as

$$\dot{\hat{\varrho}} = -\gamma(\alpha_2 + \ddot{y}_r)z_2 \quad (15)$$

and the parameter update laws are:

$$\dot{\hat{\theta}} = \Gamma \varphi z_2 \tag{16}$$

$$\dot{\hat{\beta}}_0 = -\gamma_0 \hat{z}_{f0} z_2 \tag{17}$$

$$\dot{\hat{\beta}}_1 = \gamma_1 \hat{z}_{f1} \frac{|x_2|}{g(x_2)} z_2 \tag{18}$$

$$\iota_0 = -z_2 \tag{19}$$

$$\iota_1 = \frac{|x_2|}{g(x_2)} z_2 \tag{20}$$

The design procedure in eqs. (10)-(20) results in the following error system (see Appendix: Calculations for the Error System):

$$\dot{z}_1 = -L_1 z_1 + z_2 \tag{21}$$

$$\dot{z}_2 = \varphi(x_1, x_2)^T \tilde{\theta} - z_1 - L_2 z_2 - b\tilde{\varrho}\,(\alpha_2 + \ddot{y}_r) + \frac{|x_2|}{g(x_2)} \left(\beta_1 \tilde{z}_{f1} + \tilde{\beta}_1 \hat{z}_{f1}\right) - \beta_0 \tilde{z}_{f0} - \tilde{\beta}_0 \hat{z}_{f0} \tag{22}$$

A Lyapunov function for this system is:

$$V = \frac{1}{2} z_1^2 + \frac{1}{2} z_2^2 + \frac{1}{2} \tilde{\theta}^T \Gamma^{-1} \tilde{\theta} + \frac{b}{2\gamma} \tilde{\varrho}^2 + \frac{\beta_0}{2} \tilde{z}_{f0}^2 + \frac{\beta_1}{2} \tilde{z}_{f1}^2 + \frac{1}{2\gamma_0} \tilde{\beta}_0^2 + \frac{1}{2\gamma_1} \tilde{\beta}_1^2 \tag{23}$$

Its derivative along the solution of (.3) is (see Appendix: Lyapunov Derivative.):

$$\dot{V} = -\sum_{k=1}^{2} L_k z_k^2 - \frac{|x_2|}{g(x_2)} \left(\beta_0 \tilde{z}_{f0}^2 + \beta_1 \tilde{z}_{f1}^2\right) \tag{24}$$

which proves from the Lasalle-Yoshizawa theorem that global asymptotic tracking is achieved if the error $p_{Ld} - p_L$ inside the inner loop converges to zero.

## 4. SIMULATIONS

In order to demonstrate its robustness the controller is simulated with the NHMS described in Choux and Hovland (2010) where dynamics of the valve spool and nonlinearities in the valve as well as dynamic friction in the cylinder are present. Moreover the uncertain parameters in the plant differ by up to ± 20% compared to those used in the controller design. $M^* = 0.9\,M$, $A^* = 1.1\,A$, $k^* = 0.8\,k$, $d^* = 0.8\,d$, $\sigma_2^* = 0.9\,\sigma_2$, $\sigma_1^* = 1.2\,\sigma_1$, $\sigma_0^* = 0.8\,\sigma_0$. The $*$-superscript refers to the model used by the controller.

In order to test the controller at different points of operation, the reference tracking position consists of a 5 Hz sine wave and followed by a sequence of steps between -1 and 10 mm. The controller gains choosen for the backstepping procedure are $L_1 = L_2 = 70$ and the adaptation gains are $\Gamma = \begin{bmatrix} 50 & 0 \\ 0 & 50 \end{bmatrix}$, $\gamma_0 = \gamma_1 = 50$. Position of the mass, $y$, tracking error, $z_1$ and the input voltage, $u$ are shown in Figs. 3, 4 and 5 respectively, with and without friction compensation in the controller.

Simulations are run using Matlab/Simulink with a fixed step solver of order 4 (Runge-Kutta) and 5 ms step size which is suitable for real-time implementation (for instance using National Instrument CompactRio controller, Matlab XPC Target or Siemens 300-series PLC's).

Simulation results in Fig. 4 show that the tracking error is significantly decreased with friction compensation when

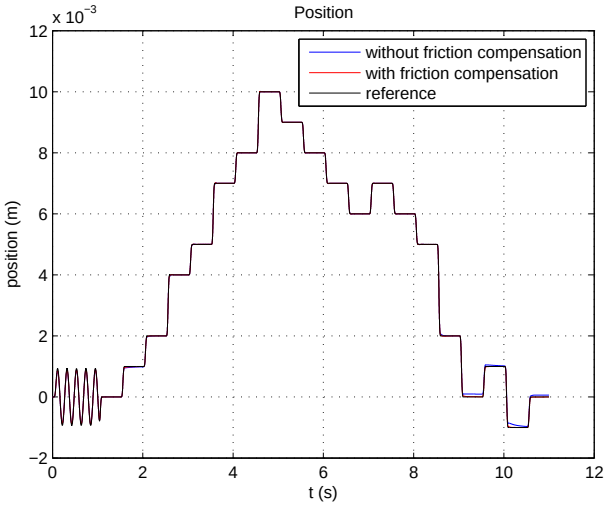


Fig. 3. Position $y$. Black, blue and red line for the reference position, the position given by the controller without and with friction compensation respectively. $L_1 = L_2 = 70$.

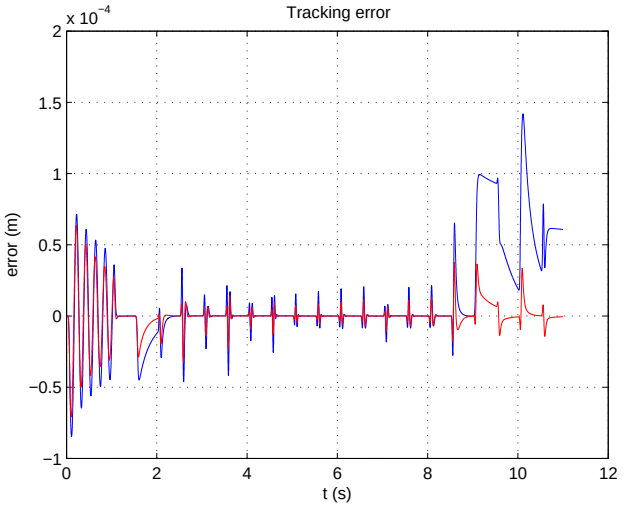


Fig. 4. Tracking error. Blue=without friction compensation, Red=with friction compensation. $L_1 = L_2 = 70$.

the operating point is close to the zero position, i.e. when the load pressure is low. It happens in the simulation at time $t = 9$ to $t = 11s$.

## 5. COMPARISON WITH FULL BACKSTEPPING

In this section the cascade controller with friction compensation developed in section 3 called CASC and the controller developed in Choux and Hovland (2010) called BS2 are compared, using the same input position reference as the previous section and same gains for the controllers. The results are shown in Figs. 6 and 7 for a similar input level (±2V).

The Mean Positioning Accuracy (MPA) and the Absolute Positioning Accuracy (APA) as defined in Bonchis et al. (2002) are shown in Table 2. The new controller CASC performs significantly better (more than a factor of 2 on both criteria), and especially for the APA improvement for positions close to zero where the load pressure is low, as

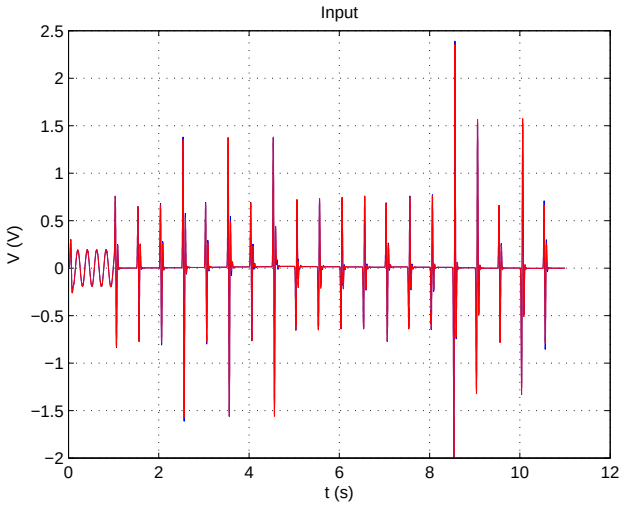


Fig. 5. Input voltage. Blue=without friction compensation, Red=with friction compensation. $L_1 = L_2 = 70$.

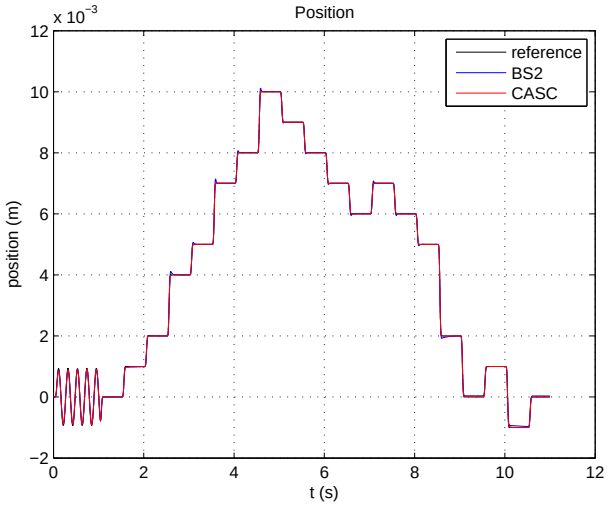


Fig. 6. Position $y$. Black, blue and red line for the reference position, the position given by the controller BS2 and CASC respectively.

| Controller Type | MPA | APA |
|---|---|---|
| BS2 (from $t = 0$ to $t = 9$) | $7.88 \cdot 10^{-4}$ | $1.71 \cdot 10^{-4}$ |
| BS2 (from $t = 9$ to $t = 11$) | $2.10 \cdot 10^{-3}$ | $1.59 \cdot 10^{-4}$ |
| CASC (from $t = 0$ to $t = 9$) | $3.90 \cdot 10^{-4}$ | $7.10 \cdot 10^{-5}$ |
| CASC (from $t = 9$ to $t = 11$) | $8.77 \cdot 10^{-4}$ | $3.64 \cdot 10^{-5}$ |
| Improvement from $t = 0$ to $t = 9$ | 2.02 | 2.41 |
| Improvement from $t = 9$ to $t = 11$ | 2.39 | 4.37 |

Table 2. Comparison of tracking performance between CASC and BS2 controller.

seen in Fig.7 (between $t = 9$ and $t = 11$). Moreover, the number of floating point operations when using controller CASC is considerably reduced compared to the BS2 and more suitable for real-time implementation, see Table 3.

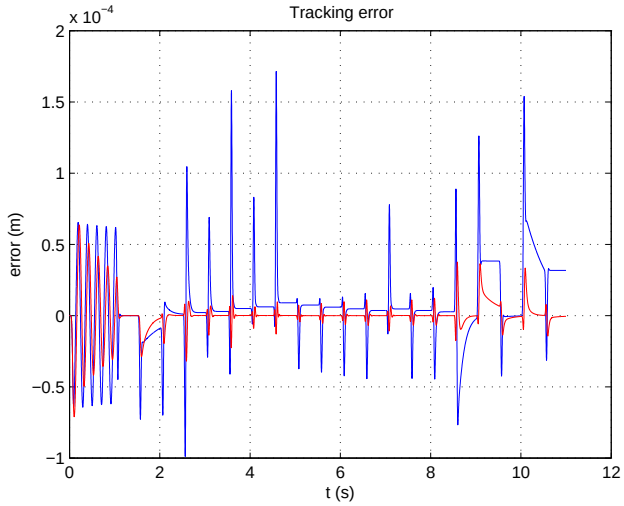


Fig. 7. Tracking error $y$. Blue and red line for the controller BS2 and CASC respectively.

| Controller Type | Costs |
|---|---|
| BS2 | $699\otimes\ 513\oplus\ 222\triangleright$ |
| CASC | $16\otimes\ 15\oplus\ 4\triangleright$ |

Table 3. Cost of BS2 and CASC optimised calculations in number of multiplication and division ($\otimes$), number of additions ($\oplus$) and number of assignments ($\triangleright$) for each control law.

## 6. CONCLUSIONS

In this paper a cascade control structure including adaptive backstepping considering a dynamic friction model for a nonlinear hydraulic-mechanical system has been developed and the performance has been compared with a similar controller without the cascade structure and the dynamic friction model. The performance criteria show that the proposed controller performs better than previous results in terms of position tracking performance when the load pressure in the cylinder is low. In addition, the complexity of the proposed control structure is reduced by a factor of 50 compared to previous results when measured in number of floating point operations, which is beneficial for real-time implementation.

Future research directions will focus on benchmarking and real-time implementation of the controller structure for an experimental nonlinear-hydraulic mechanical system as well as further theoretical analysis of the inner loop performance.

## REFERENCES

Alleyne, A. and Liu, R. (2000). Systematic control of a class of nonlinear systems with application to electrohydraulic cylinder pressure control. *IEEE Transactions on Control Systems Technology*, 8(4), 623–634. doi: 10.1109/87.852908.

Bonchis, A., Corke, P., and Rye, D. (2002). Experimental Evaluation of Position Control Methods for Hydraulic Systems. *IEEE Transactions on Control Systems Technology*, 10(6), 876–882. doi:10.1109/TCST.2002.804128.

Canudas de Wit, C., Olsson, H., Åström, K., and Lischinsky, P. (1995). A new model for control of systems with

friction. *IEEE Trans. on Automatic Control*, 40(3), 419–425. doi:10.1109/9.376053.

Choux, M. and Hovland, G. (2010). Adaptive backstepping control of nonlinear hydraulic-mechanical system including valve dynamics. *Modeling, Identification and Control*, 31(1), 35–44. doi:10.4173/mic.2010.1.3.

Kanellakopoulos, I., Kokotovic, P., and a.S. Morse (1991). Systematic design of adaptive controllers for feedback linearizable systems. *IEEE Transactions on Automatic Control*, 36(11), 1241–1253. doi:10.1109/9.100933.

Krstić, M., Kanellakopoulos, I., and Kokotović, P. (1995). *Nonlinear and Adaptive Control Design*. Wiley, New York.

Pavlichkov, S. and Ge, S. (2009). Global Stabilization of the Generalized MIMO Triangular Systems With Singular Input-Output Links. *IEEE Transactions on Automatic Control*, 54(8), 1794–1806. doi:10.1109/TAC.2009.2024566.

Schindele, D. and Aschemann, H. (2009). Adaptive friction compensation based on the LuGre model for a pneumatic rodless cylinder. *35th Annual Conf. of IEEE Industrial Electronics*, 1432–1437. doi:10.1109/IECON.2009.5414726.

Seto, D., a.M. Annaswamy, and Baillieul, J. (1994). Adaptive control of nonlinear systems with a triangular structure. *IEEE Transactions on Automatic Control*, 39(7), 1411–1428. doi:10.1109/9.299624.

Zeng, H. and Sepehri, N. (2006). Adaptive backstepping control of hydraulic manipulators with friction compensation using LuGre model. In *Proc. American Control Conference*, 3164–3169.

Zeng, H. and Sepehri, N. (2008). Tracking Control of Hydraulic Actuators Using a LuGre Friction Model Compensation. *Journal of Dynamic Systems, Measurement, and Control*, 130(1), 0145021–0145027. doi:10.1115/1.2807181.

## CALCULATIONS FOR THE ERROR SYSTEM

$$\begin{aligned}\dot{z}_1 &= \dot{x}_1 - y_r^{(1)}\\ &= x_2 - y_r^{(1)}\\ &= z_2 + \alpha_1\\ &= -L_1\, z_1 + z_2 \end{aligned} \tag{.1}$$

$$\begin{aligned}\dot{z}_2 &= \dot{x}_2 - y_r^{(2)} - \dot{\alpha}_1\\ &= \varphi(x_1,x_2)^T\theta + bu + \left(\beta_1\frac{|x_2|}{g(x_2)} - \beta_0\right) z_f - y_r^{(2)} - \dot{\alpha}_1\\ &= \varphi(x_1,x_2)^T\theta + b\hat{\varrho}\left(-z_1 - L_2 z_2 - \varphi^T\hat{\theta} + \frac{\partial\alpha_1}{\partial x_1}x_2\right.\\ &\left.+\frac{\partial\alpha_1}{\partial y_r}\dot{y}_r + \hat{\beta}_0\hat{z}_{f0} - \frac{|x_2|}{g(x_2)}\hat{\beta}_1\hat{z}_{f1} + \ddot{y}_r\right) + \frac{|x_2|}{g(x_2)}\left(\beta_1\tilde{z}_{f1}\right.\\ &\left.+\tilde{\beta}_1\hat{z}_{f1} + \hat{\beta}_1\hat{z}_{f1}\right) - \beta_0\tilde{z}_{f0} - \hat{\beta}_0\hat{z}_{f0} - \tilde{\beta}_0\hat{z}_{f0} - y_r^{(2)} - \dot{\alpha}_1\\ &= \varphi(x_1,x_2)^T\tilde{\theta} - z_1 - L_2 z_2 - b\tilde{\varrho}\,(\alpha_2 + \ddot{y}_r)\\ &+ \frac{|x_2|}{g(x_2)}\left(\beta_1\tilde{z}_{f1} + \tilde{\beta}_1\hat{z}_{f1}\right) - \beta_0\tilde{z}_{f0} - \tilde{\beta}_0\hat{z}_{f0} \end{aligned} \tag{.2}$$

## LYAPUNOV DERIVATIVE: LUGRE FRICTION MODEL

$$\begin{aligned}\dot{V} &= z_1\left(-L_1\, z_1 + z_2\right) + z_2\left(\varphi(x_1,x_2)^T\tilde{\theta} - z_1 - L_2 z_2\right.\\ &\left.-b\tilde{\varrho}\,(\alpha_2 + \ddot{y}_r) + \frac{|x_2|}{g(x_2)}\left(\beta_1\tilde{z}_{f1} + \tilde{\beta}_1\hat{z}_{f1}\right) - \beta_0\tilde{z}_{f0}\right)\\ &\left.-\tilde{\beta}_0\hat{z}_{f0}\right) + \tilde{\theta}^T\Gamma^{-1}\dot{\tilde{\theta}} + \frac{b}{\gamma}\tilde{\varrho}\dot{\tilde{\varrho}} + \beta_0\tilde{z}_{f0}\dot{\tilde{z}}_{f0} + \beta_1\tilde{z}_{f1}\dot{\tilde{z}}_{f1}\\ &+ \frac{1}{\gamma_0}\tilde{\beta}_0\dot{\tilde{\beta}}_0 + \frac{1}{\gamma_1}\tilde{\beta}_1\dot{\tilde{\beta}}_1\\ &= -\sum_{k=1}^{2} L_k\, z_k^2 + \left(z_2\varphi - \Gamma^{-1}\dot{\hat{\theta}}\right)^T\tilde{\theta}\\ &- \left(b\,(\bar{\alpha}_2 + \ddot{y}_r)\, z_2 + \frac{b}{\gamma}\dot{\hat{\varrho}}\right)\tilde{\varrho} + \left(z_2\frac{|x_2|}{g(x_2)}\beta_1\right.\\ &\left.+\beta_1\left(x_2 - \frac{|x_2|}{g(x_2)}(\tilde{z}_{f1} + \hat{z}_{f1}) - \dot{\hat{z}}_{f1}\right)\right)\tilde{z}_{f1}\\ &+ \left(z_2\frac{|x_2|}{g(x_2)}\hat{z}_{f1} - \frac{1}{\gamma_1}\dot{\hat{\beta}}_1\right)\tilde{\beta}_1\\ &+ \left(-z_2\beta_0 + \beta_0\left(x_2 - \frac{|x_2|}{g(x_2)}(\tilde{z}_{f0} + \hat{z}_{f0}) - \dot{\hat{z}}_{f0}\right)\right)\tilde{z}_{f0}\\ &+ \left(-z_2\hat{z}_{f0} - \frac{1}{\gamma_0}\dot{\hat{\beta}}_0\right)\tilde{\beta}_0\\ &= -\sum_{k=1}^{2} L_k\, z_k^2 - \beta_1\frac{|x_2|}{g(x_2)}\tilde{z}_{f1}^2 - \beta_0\frac{|x_2|}{g(x_2)}\tilde{z}_{f0}^2 \end{aligned} \tag{.3}$$